Charge Localization and Dynamics in Rhodopsin

Francesco Buda,[1] Huub J. M. de Groot,[2] and Angelo Bifone[2]
[1]*Istituto Nazionale per la Fisica della Materia, Laboratorio Forum, Scuola Normale Superiore, Piazza dei Cavalieri 7, I-56126 Pisa, Italy*
[2]*Leiden Institute of Chemistry, Gorlaeus Laboratoria, University of Leiden, 2300 RA Leiden, The Netherlands*
(Received 8 July 1996)

We present a Car-Parrinello *ab initio* molecular dynamics study of the retinylidene chromophore of rhodopsin, the membrane protein involved in the primary event in vision. We observe a coherent propagation of a conjugation defect associated with charge transport along the chromophore conjugated backbone. This solitonlike charge propagation is strongly coupled to the vibrational degrees of freedom due to the nonplanarity of the molecule. The implications for the chromophore isomerization mechanism are discussed. [S0031-9007(96)01703-6]

PACS numbers: 87.15.He, 71.15.Pd, 82.30.Qt

The cascade of biochemical reactions that is responsible for light detection and signal transduction in the visual system is initiated by the photoinduced conformational change of a 7-helix protein, rhodopsin, in the membranes of the rod cells [1]. This conformational change is triggered by the photoisomerization of a protonated Schiff base of retinal (RPSB) (Fig. 1), the chromophore of this and other important biological photoreceptors, e.g., bacteriorhodopsin, the proton-pumping protein of the *Halobacterium salinarium* [2]. The 11-*cis* to all-*trans* isomerization of the retinylidene chromophore of rhodopsin upon absorption of a photon is completed within a very short time scale (200 fs) and is one of the fastest photochemical reactions [3]. This process is characterized by a high quantum yield of 65% and by high efficiency in energy conversion, as $\approx$60% of the energy of the photon is stored in the primary photoproduct, bathorhodopsin, a highly strained all-*trans* form of the retinylidene chromophore [1].

In this Letter, we study the dynamics of a RPSB, including the most relevant interactions with the host protein, within an *ab initio* Car-Parrinello molecular dynamics framework [4]. This approach allows us to study the electron charge density rearrangement coupled to chain deformations and vibrational motion of the conjugated backbone. We show that the RPSB supports a propagating conjugation defect, which may drive the photoisomerization and determine the remarkable performance of this molecular device [5,6]. The propagating conjugation defect carries the charge along the conjugated backbone. This solitonlike coherent charge propagation is strongly coupled to the vibrational degrees of freedom, due to the nonplanarity of the chromophore.

Previous density functional theory (DFT) in local density approximation [7] studies in infinite polyacetylene chains have suffered from the poor description of the dimerization [8], which precluded an *ab initio* approach to soliton dynamics. In retinals, however, the bond alternation is determined by the asymmetry of the molecule, and is stabilized by the β-ionone ring, the side methyl groups, and the highly electrophylic tail. Recently, we have shown that the Car-Parrinello method provides an excellent framework to study such short conjugated chains [9].

The *ab initio* molecular dynamics approach describes the Newtonian dynamics of a system by using an interatomic potential obtained at each time step from the instantaneous electronic ground state computed within the DFT [4]. Gradient corrections to the exchange-correlation functional have been included in the form proposed by Becke [10] and Perdew [11]. We explicitly treat only the valence electrons and describe the interaction with the inner core by using soft first-principles pseudopotentials [12]. The Kohn-Sham single particle wave functions are expanded on a plane wave basis set with an energy cutoff of 20 Ry. The convergence of the calculation relative to the energy cutoff has been tested on a C_2H_6 and a HCN molecule up to 30 Ry. At 20 Ry the C-C and C-N bond lengths are already close to the fully converged values within $\approx$1.0%. The C-C and the C-N stretch frequencies are accurate within $\approx$1.0% and $\approx$2.0%, respectively. The expansion in terms of plane waves implies the use of periodic boundary conditions. The simulation box has been chosen large enough to avoid interaction with the images, specifically $36 \times 22 \times 22$ au. The time step for the molecular dynamics simulations is 0.15 fs.

The geometric and electronic structures of the retinal chromophore in rhodopsin are sensitive to the interactions with the protein, which ultimately determines the

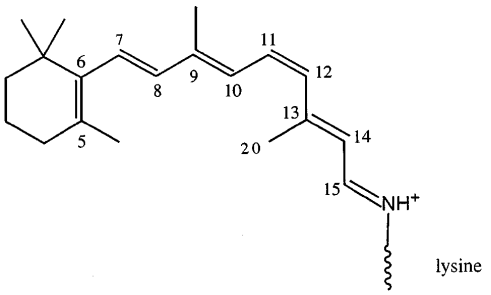

FIG. 1. Schematic representation of the 11-*cis* retinal protonated Schiff base.

 0031-9007/96/77(21)/4474(4)$10.00 © 1996 The American Physical Society

function of the RPSB. The steric hindrance of the methyl group bound to C13 with the protein residues induces a twist of the C12-C13 bond, and a consequent out-of-plane distortion of the chromophore, which affects the mechanism and the quantum efficiency of the isomerization process [13]. We have modeled the chromophore starting with initial C20-C11 and C20-C10 distances of 3.0 and 3.05 Å,respectively, as determined by recent solid state NMR experiments [13]. The chromophore has been terminated with a CH_2-CH_3 group to mimic the linkage to the protein lysine. The protonation of the retinal-lysine Schiff base adds a net positive charge to the chromophore. Two-photon absorption studies indicate a neutral binding site [14], which implies a negatively charged counterion in the close vicinity of the chromophore. Mutagenesis experiments in bacteriorhodopsin have demonstrated that the interaction with charged protein residues determines the high photoisomerization rate of the chromophore [15]. In our simulation, the counterion has been modeled by including a chlorine ion (Cl^-) placed at $\approx$4 Å from C12. Although much simpler than the actual counterion identified with a glutamate protein residue [16], this counterion captures the essential electrostatic interaction, as shown in Ref. [17].

The ground state equilibrium structure of the RPSB has been determined by a simulated annealing procedure [4]. During the molecular dynamics, the terminal CH_2-CH_3 group and the counterion have been fixed, as no major changes in the protein conformation have to be expected on the time scale of the photoisomerization. We have also fixed the carbon atoms of the methyl groups bound to C9 and C13. In fact, experimental evidence of steric interactions of these methyl groups with protein residues supports the model of a tight binding pocket, where methyl group oscillations are hindered [13]. The optimized C20-C11 and C20-C10 distances do not substantially differ from the initial values and are 3.05 and 3.08 Å, respectively. The backbone of the RPSB presents clear bond alternation except for the terminal region C12-C13-C14 (Table I). For comparison we have also optimized the structures of the 11-*cis* retinal and of the unprotonated Schiff base, which do not bear any net charge. As apparent from Table I, these systems present a bond alternation along the entire backbone. Thus, we conclude that the excess positive charge borne by the chromophore induces a dimerization defect, which is located in proximity of the nitrogen atom (Table I). In Fig. 2 we show the difference between the electron charge distribution of the RPSB and the unprotonated retinal Schiff base. The charge difference has the opposite sign on adjacent C-C bonds, and decays in going from the N towards the ring. These charge oscillations are typical of a charged defect in a conjugated chain and have been revealed in rhodopsin, diphenylpolyenyl anions, and doped polyacetylene fragments by ^{13}C NMR [17–19]. The charge oscillations of Fig. 2 correlate with the differences in the backbone C-C bond lengths between the positively charged and the neutral retinal Schiff base (see Table I). The conjugation defect is delocalized over several bonds, with a half-width of approximately two bonds, to be compared with five bonds in the Su-Schrieffer-Heeger solution for a charged soliton in an infinite chain of polyacetylene [20]. Optimization of the structure without the negative chlorine ion yields a more delocalized positive charge on the retinal backbone.

Starting from the structure of rhodopsin, the hydrogen atom bound to C12 has been flipped into a *trans* position with respect to the hydrogen of C11. This induces a severe strain of the backbone. When the system in such a highly distorted all-*trans* configuration is allowed to evolve in a microcanonical molecular dynamics simulation, the backbone readjusts to release the strain. The potential energy stored in the retinal is transferred into kinetic energy of the atoms and a coherent propagation of the positively charged conjugation defect along the backbone is observed. This propagation induces an inversion of the single-double bond alternation, in the fashion of a positively charged soliton. This analogy makes it natural to compare the conjugation defect in RPSB to a soliton, although the concept of soliton is rigorously defined only for an infinite conjugated chain. Figure 3 shows the time dependence of the dimerization

TABLE I. Computed carbon-carbon bond lengths (in Å) for the optimized structures of RPSB, including the Cl^- counterion (rhodopsin); bathorhodopsin, including the Cl^- counterion; 11-*cis* isomer of retinal [9]; unprotonated 11-*cis* Schiff base of retinal (RSB).

Bond	Rhodopsin	Bathorhodopsin	11-*cis* Retinal	RSB
C5═C6	1.370	1.376	1.371	1.370
C6—C7	1.460	1.445	1.452	1.460
C7═C8	1.367	1.380	1.366	1.367
C8—C9	1.442	1.425	1.442	1.442
C9═C10	1.388	1.402	1.380	1.388
C10—C11	1.422	1.402	1.425	1.422
C11═C12	1.389	1.400	1.376	1.389
C12—C13	1.423	1.407	1.448	1.445
C13═C14	1.406	1.420	1.375	1.378
C14—C15	1.391	1.383	1.443	1.453
C15═N	1.342	1.359		1.294

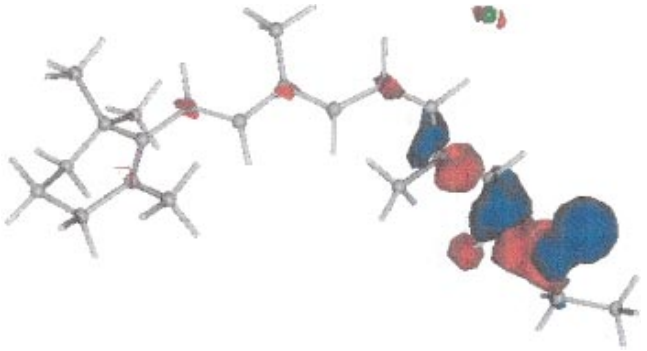

FIG. 2(color). Difference between the electron charge distribution of the protonated and unprotonated retinal Schiff base. The red and blue isosurfaces correspond to electron density differences of $+0.005$ and $-0.005\ e/\text{au}^3$, respectively. The color alternation reflects the charge density oscillations along the conjugated backbone induced by the positively charged defect. The green ball represents the Cl^- ion.

amplitudes (defined as the difference between adjacent C-C bond lengths) at various positions along the backbone. An inversion of the bond order in this representation corresponds to a change of sign in the dimerization amplitudes. An inversion in the bond alternation for the C12-C13 and C13-C14 bonds occurs after about 20 fs, followed by an inversion for C10-C11 and C11-C12, and for C8-C9 and C9-C10, after 35 and 40 fs, respectively. Figure 4 shows two snapshots of the electronic charge density of the highest occupied molecular orbital (HOMO) at the beginning of the molecular dynamics simulation and after 65 fs, when the inversion of bond order is complete. The displacement of the positive charge towards the ring is apparent. Thus, charge propagation is intimately associated with propagation of the conjugation defect. The defect is reflected by the ionon ring and, similarly, at the Schiff base end, thus being confined in the region C6-C15. By timing the inversion of bond alternation pattern, we estimate a velocity for the propagation of the charged defect of 1.4 $(\pm 0.4) \times 10^6$ cm/sec.

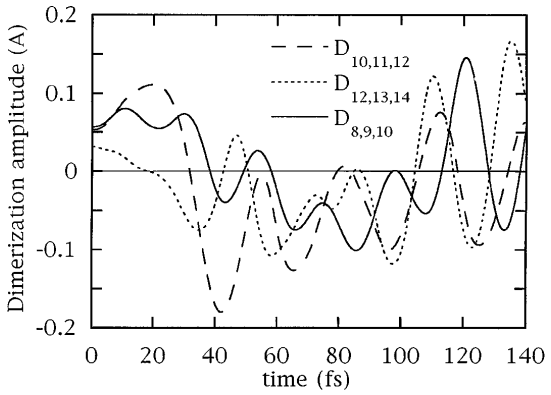

FIG. 3. Dimerization amplitudes (defined as the difference between adjacent C-C bond lengths) as a function of time during the molecular dynamics simulation. $D_{i,j,k} = d_{i,j} - d_{j,k}$, where $d_{i,j}$ denotes the length of the bond between C atoms i and j. The C6-C7 and C7-C8 bonds are also affected during the dynamics, but an inversion of bond order is never observed.

An analysis of the dihedral H-C-C-H and C-C-C-C angles in the region C9-C10-C11-C12 shows that the defect propagation is strongly coupled to out-of-plane oscillations of the molecule. This causes a transfer of energy into vibrational modes, with a consequent damping and loss of coherence of the defect propagation. The strong oscillations of the hydrogen atoms bound to C11 and C12 upon the passage of the defect corroborates the idea that a propagating coherent excitation drives the isomerization of the chromophore [5,6].

Because of the low symmetry of the molecule, the vibrational spectra of retinals are dominated by highly localized vibrational modes [9,21]. In the RPSB, however, an analysis of the atomic trajectories during the simulation [9] reveals a low frequency collective vibrational feature at $\approx 270\ \text{cm}^{-1}$, which can be related to the soliton propagation. Thus, the charge oscillation is associated with a collective slow mode, which arises from the coupling of the soliton propagation along the backbone to torsional modes of the chain. These results are consistent with resonance Raman spectroscopy data [22], which show intense low-frequency Raman lines at 249 and 262 cm^{-1}. After 250 fs of simulation within a microcanonical dynamics, we have cooled down the system with a simulated annealing procedure. In the equilibrium structure of the final distorted all-*trans* configuration

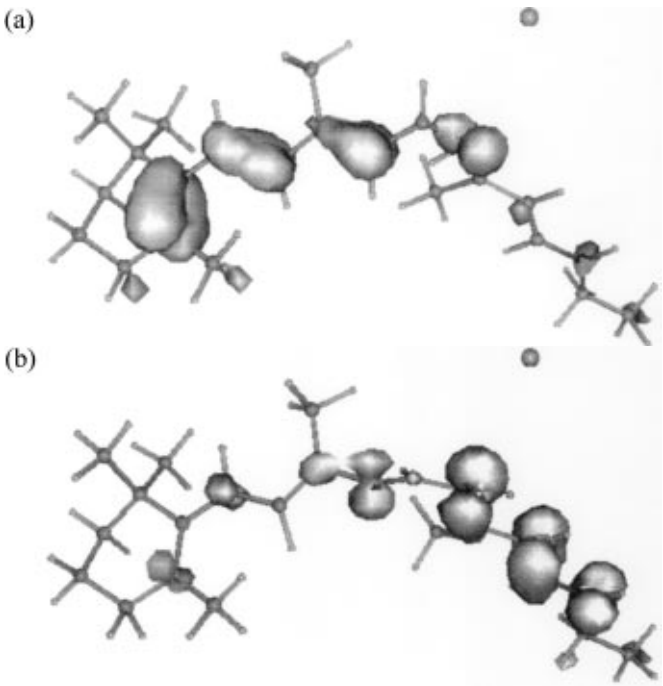

FIG. 4. Electron charge distribution of the HOMO (a) immediately after flipping the hydrogen atom to a *trans* position and (b) after 65 fs of molecular dynamics (same visualization criteria as Fig. 2). Remarkably, the charge distribution in (b) is similar to the charge distribution of the lowest unoccupied molecular orbital in the 11-*cis*-RPSB and mimics the polarization of the RPSB upon excitation [23].

(bathorhodopsin), the positive charge and the associated conjugation defect are still located in proximity of the nitrogen atom, although more delocalized than in the 11-*cis* RPSB (see Table I).

The effective mass M_s of a charged soliton is normally computed from the equation

$$E_{\mathrm{kin}} = \frac{1}{2} M_s v_s^2 , \tag{1}$$

where v_s is the velocity of propagation and E_{kin} is the sum of the kinetic energies of the atoms involved in the soliton domain. For an infinite polyene chain, the Su-Schrieffer-Heeger model [20] yields a mass M_s of ≈ 6 electron masses, much lighter than the mass of a carbon atom. In our three-dimensional model, the computation of the soliton mass is less straightforward, as the defect propagation excites vibrational modes. The incoherent exchange of energy with the vibrations prevents an analysis in terms of the kinetic energies of the carbon groups in the soliton domain, as they also include contributions from the thermally excited vibrational modes. Moreover, the charge oscillation along the backbone is associated with a collective torsional mode, which is coherent with the soliton propagation. An alternative way to assign a mass to this "dressed soliton" is considering the energy of the slow mode associated with the soliton propagation as kinetic energy in Eq. (1). This procedure yields a soliton mass M_s of the order of 100 electron masses. We expect the mass of the soliton to depend on the molecule conformation and on the length of the chain, and not to be a universal characteristic for this sort of systems.

The dynamics of the positively charged defect is independent of the constraints that are imposed to the molecule. A molecular dynamics simulation where the side methyl groups are not fixed yields qualitatively analogous results. In fact, the time scales of the motion of the methyl groups and of the rearrangement of the backbone in a linear all-*trans* form are much longer than the propagation of the soliton.

In conclusion, we have studied for the first time the dynamics of a positively charged defect along the backbone chain of a RPSB within a Car-Parrinello *ab initio* molecular dynamics approach. The soliton dynamics in this system is strongly coupled to out-of-plane hydrogen oscillations, and may be relevant for the photoisomerization of the chromophore of rhodopsin [5,6]. The nonplanarity of the molecule, determined by the interaction of the side methyl groups with the binding pocket, induces a strong coupling of the charge oscillations along the conjugated backbone to the vibrational degrees of freedom. This coupling causes incoherent energy transfer to vibrations when the soliton passes through the twisted region of the molecule. This observation supports the idea that the steric interaction with the protein is crucial to the function of the chromophore [13]. In fact, multiple passages of the excitation in the region of the twist may cause back-isomerization processes; thus, a rapid damping of the soliton is crucial to ensure high quantum yield.

We thank J. Shelley for the graphic package (MOVIE) used to visualize the results of the simulations. We are grateful to J. Lugtenburg for his constant support and encouragement and J. Zaanen, F. L. J. Vos, D. P. Aalberts, W. van Saarloos, and A. Curioni for interesting discussions. The numerical calculations were performed in the Computer Center of the Scuola Normale Superiore in Pisa, Italy. Research partially supported by the EC Biotechnology program, Contract No. CT930467.

[1] R. R. Birge, Biochim. Biophys. Acta **1016**, 293 (1990).
[2] J. Lugtenburg, R. A. Mathies, R. G. Griffin, and J. Herzfeld, TIBS **13**, 388 (1988).
[3] R. W. Schoenlein, L. A. Petenau, R. A. Mathies, and C. V. Shank, Science **254**, 412 (1991).
[4] R. Car and M. Parrinello, Phys. Rev. Lett. **55**, 2471 (1985).
[5] F. L. J. Vos, D. P. Aalberts, and W. van Saarloos, Phys. Rev. B **53**, 14 922 (1996).
[6] D. S. Chernavskii, FIAN Report No. 295, Moscow, 1986.
[7] See, e.g., R. G. Parr and W. Yang, *Density-Functional Theory of Atoms and Molecules* (Oxford University Press, New York, 1989).
[8] J. W. Mintmire and C. T. White, Phys. Rev. B **35**, 4180 (1987); P. Vogl and D. K. Campbell, Phys. Rev. Lett. **62**, 2012 (1989); J. Ashkenazi, W. E. Pickett, H. Krakauer, C. S. Wang, B. M. Klein, and S. R. Chubb, Phys. Rev. Lett. **62**, 2016 (1989).
[9] A. Bifone, H. J. M. de Groot, and F. Buda, Chem. Phys. Lett. **248**, 165 (1996).
[10] A. D. Becke, Phys. Rev. A **38**, 3098 (1988).
[11] J. P. Perdew, Phys. Rev. B **33**, 8822 (1986).
[12] D. Vanderbilt, Phys. Rev. B **41**, 7892 (1990).
[13] P. Verdegem, P. Bovee-Geurts, W. de Grip, J. Lugtenburg, and H. J. M. de Groot (to be published).
[14] R. R. Birge, L. P. Murray, P. M. Pierce, H. Akita, V. Balogh-Nair, L. A. Findsen, and K. Nakanishi, Proc. Natl. Acad. Sci. U.S.A. **82**, 4117 (1985).
[15] L. Song, M. A. El-Sayed, and J. K. Lanyi, Science **261**, 891 (1993).
[16] T. P. Sakmar, R. R. Franke, and H. G. Khorana, Proc. Natl. Acad. Sci. U.S.A. **86**, 8309 (1989).
[17] M. Han, S. DeDecker, and S. O. Smith, Biophys. J. **65**, 899 (1993).
[18] L. M. Tolbert, Acc. Chem. Res. **25**, 561 (1992).
[19] L. M. Tolbert and M. E. Ogle, J. Am. Chem. Soc. **112**, 9519 (1990).
[20] W. P. Su, J. R. Schrieffer, and A. J. Heeger, Phys. Rev. B **22**, 2099 (1980).
[21] B. Curry, I. Palings, A. D. Broek, J. A. Pardoen, J. Lugtenburg, and R. A. Mathies, in *Advances in Infrared and Raman Spectroscopy*, edited by R. J. H. Clark and R. E. Hoester (Wiley, Heyden, 1985), Vol. 12, p. 115.
[22] G. R. Loppnow and R. A. Mathies, Biophys. J. **54**, 35 (1988).
[23] R. Mathies and L. Stryer, Proc. Natl. Acad. Sci. U.S.A. **73**, 2169 (1976).